Taylor & Francis
Taylor & Francis Group

ORIGINAL RESEARCH

GUCY2C-directed CAR-T cells oppose colorectal cancer metastases without autoimmunity

Michael S. Magee[a,b], Crystal L. Kraft[b], Tara S. Abraham[b], Trevor R. Baybutt[b], Glen P. Marszalowicz[c], Peng Li[d], Scott A. Waldman[b], and Adam E. Snook [b]

aBluebird Bio, Seattle, Cambridge, MA, USA; bDepartment of Pharmacology and Experimental Therapeutics, Thomas Jefferson University, Philadelphia, PA, USA; cSchool of Biomedical Engineering, Science & Health Systems, Drexel University, Philadelphia, PA, USA; dDepartment of Pathology, Stanford University School of Medicine, Stanford, CA, USA

ABSTRACT

Adoptive T-cell therapy (ACT) is an emerging paradigm in which T cells are genetically modified to target cancer-associated antigens and eradicate tumors. However, challenges treating epithelial cancers with ACT reflect antigen targets that are not tumor-specific, permitting immune damage to normal tissues, and preclinical testing in artificial xenogeneic models, preventing prediction of toxicities in patients. In that context, mucosa-restricted antigens expressed by cancers exploit anatomical compartmentalization which shields mucosae from systemic antitumor immunity. This shielding may be amplified with ACT platforms employing antibody-based chimeric antigen receptors (CARs), which mediate MHC-independent recognition of antigens. GUCY2C is a cancer mucosa antigen expressed on the luminal surfaces of the intestinal mucosa in mice and humans, and universally overexpressed by colorectal tumors, suggesting its unique utility as an ACT target. T cells expressing CARs directed by a GUCY2C-specific antibody fragment recognized GUCY2C, quantified by expression of activation markers and cytokines. Further, GUCY2C CAR-T cells lysed GUCY2C-expressing, but not GUCY2C-deficient, mouse colorectal cancer cells. Moreover, GUCY2C CAR-T cells reduced tumor number and morbidity and improved survival in mice harboring GUCY2C-expressing colorectal cancer metastases. GUCY2C-directed T cell efficacy reflected CAR affinity and surface expression and was achieved without immune-mediated damage to normal tissues in syngeneic mice. These observations highlight the potential for therapeutic translation of GUCY2C-directed CAR-T cells to treat metastatic tumors, without collateral autoimmunity, in patients with metastatic colorectal cancer.

Abbreviations: ACT, adoptive cell therapy; CAR, chimeric antigen receptor; GFP, green fluorescent protein; GUCY2C, guanylyl cyclase C; TBI, total body irradiation

Introduction

Colorectal cancer (CRC) is the fourth leading cause of cancer, and the second leading cause of cancer-related death in the United States and world.[1] While surgical excision of primary tumors can be curative, particularly at the earliest stages of disease, about 50% of patients with colorectal cancer ultimately die of distant metastases.[1] While chemo-, radio-, and targeted therapies extend survival to about 24 mo, less than 15% of patients with metastatic CRC survive beyond 5 y,[1] highlighting the unmet need for new therapeutic paradigms for this disease.

Adoptive T-cell therapy (ACT) is an emerging platform[2] to treat patients with advanced cancer employing autologous tumor-specific T cells that are expanded *ex vivo* and transferred back into patients. While initial approaches employed tumor-infiltrating lymphocytes (TILs) to treat melanoma,[3] genetic modification of bulk peripheral blood T cells to express antigen-specific receptors theoretically extends this approach to all cancers, with notable success in treating leukemia and neuroblastoma.[4-6] However, ACT has had limited utility against epithelial tumors, reflecting unresolved issues surrounding toxicities. Indeed, employing receptors directing genetically modified T cells to target antigens that are shared by tumors and normal tissues can produce severe autoimmune damage and patient death.[7,8] Moreover, ACT products examined clinically have been tested in preclinical mouse models devoid of endogenous target antigen, incompletely characterizing the potential for toxicities in normal tissues.[9,10] In that context, T cells engineered to express an affinity-enhanced TCR targeting the colorectal tumor antigen carcinoembryonic antigen (CEA), also broadly expressed by intestinal epithelial cells, produced severe colitis in patients.[8] Similarly, T cells modified to express an antibody-based chimeric antigen receptor (CAR) targeting the tumor antigen ERBB2 (Her-2) produced lethal pneumonitis in the only patient receiving this therapy,
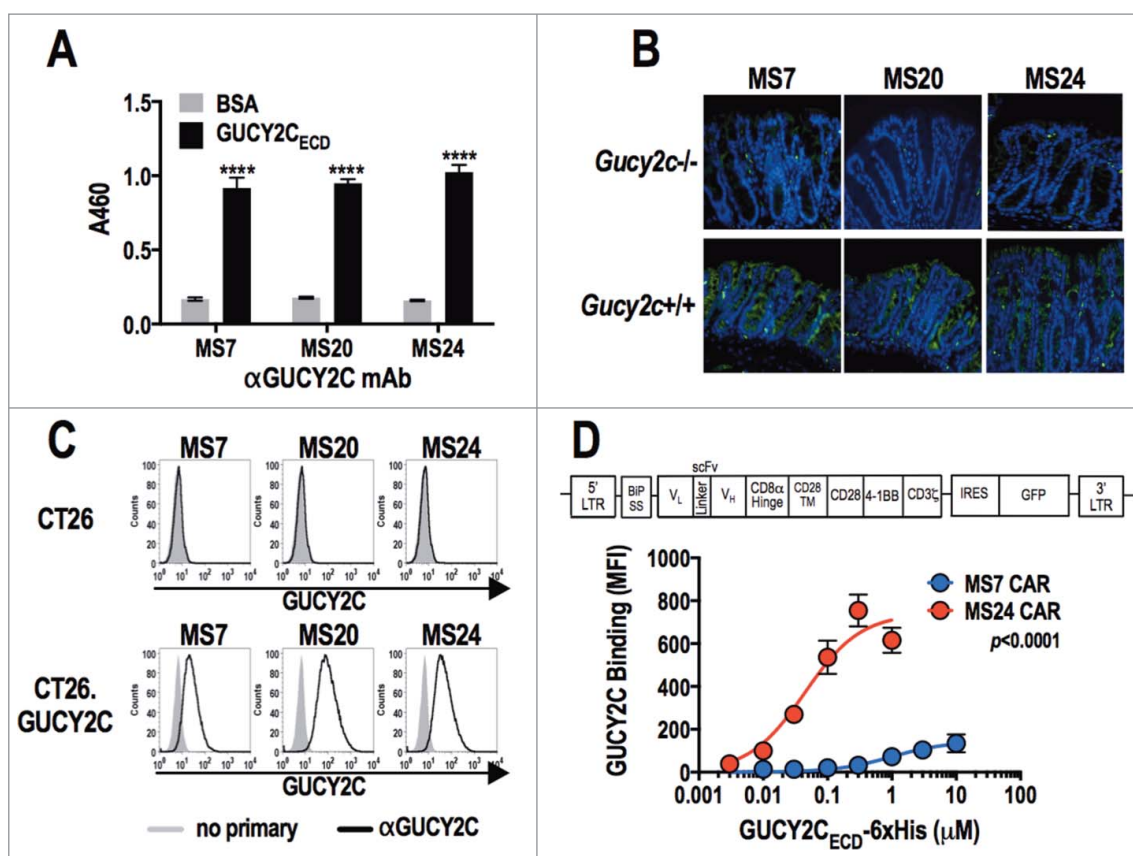
Figure 1. Characterization of GUCY2C-specific antibodies and CAR constructs. (A) Monoclonal antibodies generated against GUCY2C (MS7, MS20, and MS24) were assessed by ELISA for specific binding to GUCY2C$_{ECD}$ or negative control bovine serum albumin (BSA) plated at 1 μg/mL, ****$p < 0.0001$ (Two-way ANOVA of GUCY2C vs. BSA – binding for each mAb). (B) Wild-type (*Gucy2c*$^{+/+}$) or GUCY2C-deficient (*Gucy2c*$^{-/-}$) mouse colon sections were stained with GUCY2C-specific monoclonal antibodies (*green*), demonstrating specificity of antibodies for GUCY2C in the intestine. DAPI (*blue*). Representative of three sections each. (C) Flow cytometry analysis was performed on GUCY2C-deficient (CT26) and GUCY2C-expressing (CT26.GUCY2C) CT26 mouse colorectal cancer cells stained with GUCY2C mAbs. Results are representative of two experiments. (D) A third generation CAR construct was synthesized containing the BiP signal sequence, scFv, the CD8α hinge region, the transmembrane and intracellular domain of CD28, the intracellular domain of 4-1BB (CD137) and the intracellular domain of CD3ζ. The CAR construct was inserted into the MSCV retroviral plasmid pMIG upstream of an IRES-GFP marker. (D) Murine CD8$^+$ T cells transduced with a retrovirus containing a Control CAR or CARs derived from GUCY2C antibodies (MS7 and MS24) were labeled with varying concentrations of purified 6xHis-GUCY2C$_{ECD}$ (0–10 μM) detected with α5xHis-Alexa-647 conjugate. Flow plots (Fig. S3) were gated on live CD8$^+$ cells and the mean fluorescence intensity (MFI) indicated 6xHis-GUCY2C$_{ECD}$ binding on live CD8$^+$ transduced (GFP$^+$) cells. MS7 and MS24 binding curves were compared by extra-sum-of-squares F test. Data represent mean ± standard deviation of three experiments.

reflecting Her-2 expression in lung.[7] These considerations highlight the importance of identifying tumor-selective antigens, immune cell platforms that optimally discriminate tumor and normal tissues, and syngeneic preclinical models to define the biology, efficacy, and safety of new ACT paradigms.[11-13]

Guanylyl cyclase C (GUCY2C) is a membrane-bound cyclase whose cell-surface expression is confined to the apical surfaces of intestinal epithelial cells and exhibits limited expression in extra-intestinal tissues of humans and mice.[14,15] Of significance, GUCY2C is a cancer mucosa antigen,[16] universally overexpressed by primary and metastatic human CRCs and is ectopically expressed in esophageal and gastric cancers associated with intestinal dysplasia.[14,15,17,18] Moreover, anatomical segregation of GUCY2C on the luminal surface of the intestinal epithelium[19-22] limits access to systemically delivered GUCY2C-targeted molecules permitting diagnostic imaging[23] and monoclonal antibody-based therapy[24,25] of colorectal cancer metastasis without recognition of intestinal epithelium. Further, GUCY2C vaccines induce CD8$^+$ T cell and antibody responses that eliminate metastatic colorectal tumors, without autoimmunity, in syngeneic mouse models[26-28] and this platform is currently being tested in humans.[29]

Beyond vaccines, luminal compartmentalization of GUCY2C offers an intriguing solution to toxicities of current ACT paradigms against metastatic CRC. Moreover, a syngeneic mouse model, in which endogenous target antigen expression in normal tissue and tumors closely models humans, offers a unique opportunity to directly test CAR-T cell therapeutic efficacy and toxicity. The present study examined the ability of CAR-T cells directed to murine GUCY2C to treat established parenchymal CRC metastases without autoimmunity. This study establishes proof-of-principle for safe and effective GUCY2C CAR-T cell therapy, which can be translated to CRC patients.

Results

GUCY2C CAR-T cells

Monoclonal antibodies targeting the GUCY2C extracellular domain (GUCY2C$_{ECD}$) generated from hybridomas (MS7, MS20, and MS24) recognized purified GUYC2C (Fig. 1A), GUCY2C in the colon (Fig. 1B), and small intestine (Fig. S1) of *Gucy2c*$^{+/+}$, but not *Gucy2c*$^{-/-}$, mice; and GUCY2C-expressing, but not GUCY2C-deficient, CT26 murine colorectal cancer cells (Fig. 1C).
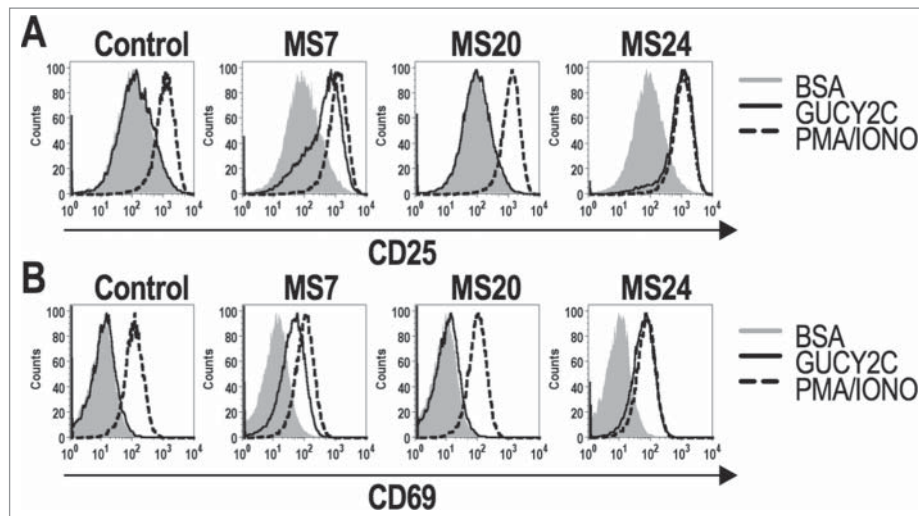
Figure 2. GUCY2C-specific CARs mediate antigen-dependent T cell activation. 1×10^6 CAR-expressing T cells were stimulated for 6 h with plate-coated antigen (BSA or GUCY2C) or PMA and Ionomycin (PMA/IONO). T cell activation markers CD25 (A) and CD69 (B) were quantified by flow cytometry. Histograms are gated on live CD8$^+$GFP$^+$ T cells. Results are representative of three experiments.

Heavy and light chain variable region sequences from each of the GUCY2C-specific hybridomas were used to generate third-generation CARs (Fig. 1D), which were inserted into a retroviral construct used to infect T cells with ˜65% transduction efficiencies (Fig. S2). GUCY2C-binding avidity was quantified by incubating CAR-T cells with increasing concentrations of purified 6xHis-tagged GUCY2C$_{ECD}$, followed by detection with labeled α6xHis antibody and assessment by flow cytometry (Fig. 1D and Fig. S3). GUCY2C binding was detected with constructs derived from the MS7 and MS24, but not MS20, antibodies. CARs derived from MS24 exhibited ˜22-fold greater avidity (K_{av} 44.3 nM vs. 994.2 nM; $p = 0.0567$) and ˜5-fold greater surface expression (B_{max} 741.5 vs. 144.2; $p < 0.0001$) compared to MS7-derived CARs (Fig. 1D), similar to the higher avidity of MS24 monoclonal antibody in comparison to MS7 (Fig. S4).

GUCY2C CARs mediate antigen-specific activation of T cells

MS7 and MS24, but not MS20 or control, CAR-T cells upregulated CD25 and CD69[30] when stimulated with immobilized GUCY2C$_{ECD}$, but not BSA (Fig. 2). All T cells produced comparable levels of CD25 and CD69 when stimulated with PMA and ionomycin, confirming that transduction with different CARs did not impact T cell activation. MS24 CAR mediated greater activation than MS7 CAR (Fig. 2), consistent with its ˜22-fold higher avidity (Fig. 1D). MS20 CAR was excluded from further consideration reflecting its inability to bind GUCY2-C$_{ECD}$ (Fig. S3) or mediate GUCY2C-dependent T cell activation (Fig. 2). MS7 and MS24, but not control, CAR-T cells produced effector cytokines IFNγ, TNFα, and MIP-1α when stimulated with immobilized GUCY2C$_{ECD}$, but not BSA (Fig. 3). Importantly, MS24 CAR-T cells exhibited greater polyfunctionality than MS7 CAR-T cells (Fig. 3B) characterized by a reduction in cells producing no cytokines ($p < 0.0001$, Two-way ANOVA) and an increase in cells producing two or three cytokines ($p < 0.05$ and $p < 0.0001$, respectively, Two-way ANOVA) following GUCY2C stimulation. Similarly, MS7 and MS24, but not control, CAR-T cells lysed GUCY2C-expressing, but not GUCY2C-deficient, CT26 mouse colon cancer cells

(Fig. 4). As expected, MS24 CAR T cells lysed GUCY2C-expressing CT26 cells more rapidly than MS7 CAR-T cells (half-maximal lysis at 54 min vs. 200 min; $p < 0.05$; Figs. 4B and D) consistent with its higher avidity (Fig. 1D).

GUCY2C CAR-T cells oppose metastatic colorectal cancer

Mice received CT26.GUCY2C cells by tail vein to induce lung metastases,[31] followed 3 d later by 5 Gy total body irradiation (TBI) and 1×10^7 T cells.[32] A non-myeloablative dose of 5 Gy TBI was administered prior to T cell transfer to enhance the efficacy of adoptive T cell therapy by reducing sinks for the homeostatic cytokines IL-7 and IL-15.[33,34] The number of tumors in lungs of mice treated with GUCY2C CAR-T cells was significantly reduced compared to mice treated with control CAR-T cells (Figs. 5A and B). Moreover, GUCY2C CAR-T cell-treated mice exhibited reduced morbidity, quantified by cachexia (Fig. 5C), and improved survival (Fig. 5D). As expected, morbidity (Fig. 5C) and survival (Fig. 5D) were significantly better with MS24, compared to MS7, CAR-T cells.

GUCY2C CAR-T cells do not induce autoimmunity

MS24 CAR-T cells produce the greatest GUCY2C-dependent T cell activation (Fig. 2), cytokine production (Fig. 3), cytolysis (Fig. 4), and antitumor efficacy (Fig. 5) without autoimmunity (Fig. 6). Mice receiving MS24 CAR-T cells were healthy with no signs or symptoms of inflammatory bowel disease including failure to thrive, altered bowel habits, or rectal bleeding. MS24 CAR-T cells accumulated in GUCY2C-expressing CT26 lung metastases (Figs. 6A and B), mediating antitumor immunity (Fig. 5), but were absent from intestines (Figs. 6A and B), producing no T cell-mediated damage quantified by histopathology (Figs. 6C and D). Similarly, MS24 CAR-T cell-treated mice were free of immune-mediated damage in extra-intestinal tissues by histopathology (Fig. 6D) and exhibited normal organ and metabolic functions quantified by serum chemistries (Fig. S5).
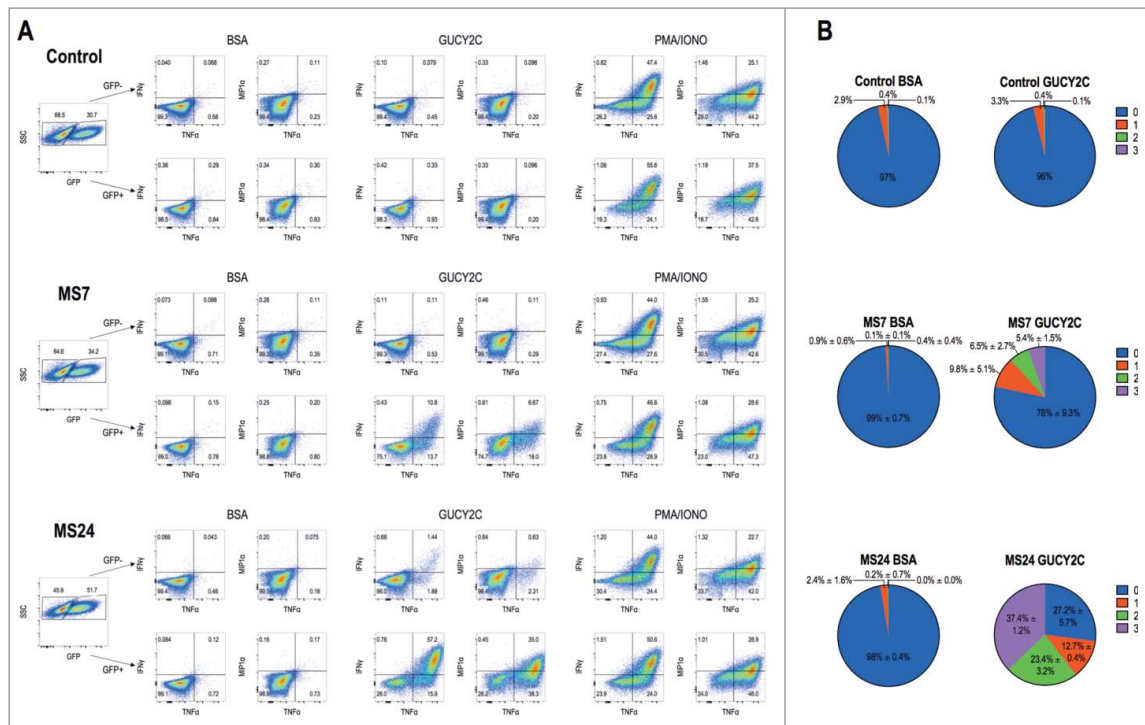
Figure 3. GUCY2C-specific CARs mediate cytokine production. 1×10^6 CAR-expressing T cells were stimulated for 6 h with plate-coated antigen (BSA or GUCY2C) or PMA and Ionomycin (PMA/IONO) in the presence of protein transport inhibitor. Cells were fixed, permeabilized, and stained for the intracellular cytokines IFNγ, TNFα, or MIP-1α and analyzed via flow cytometry. (A) Plots are gated on live GFP- (top) or GFP+ (bottom) CD8$^+$ T cells. (B) Polyfunctional cytokine graphs depict the percentages of CAR-T cells producing 0, 1, 2, or 3 cytokines. Plots in (A) are representative of two experiments, and polyfunctional cytokine analysis (B) represent means ± standard deviation of two experiments.

Discussion

This study provides the first proof-of-principle for GUCY2C CAR-T cells to treat parenchymal colorectal cancer metastases without autoimmunity in a syngeneic mouse model. Immunologic competence of GUCY2C CARs was reflected by the ability of GUCY2C, but not control, CAR-T cells to engage GUCY2C and induce T cell activation (Fig. 2) and effector function (Figs. 3 and 4). Immunologic competence was associated with the ability of GUCY2C, but not control, CAR-T cells to induce GUCY2C-dependent cytokine production (Fig. 3) and in vitro colorectal cancer cell cytolysis (Fig. 4). Further, GUCY2C, but not control, CAR-T cells reduced disease burden, improved morbidity, and produced durable eradication of disease in a mouse model of GUCY2C-expressing colorectal cancer metastases in lung (Fig. 5). Moreover, therapeutic efficacy was achieved without immune-mediated tissue damage, in small and large intestine or other extra-intestinal tissues (Fig. 6 and Fig. S5). Importantly, the superior therapeutic efficacy and safety of GUCY2C CAR-T cells was achieved in a syngeneic mouse model in which GUCY2C was endogenously expressed in normal tissues in a pattern recapitulating that in humans, colorectal tumors expressed an identical antigen, and T cells were directed by CAR receptors to that endogenous antigen. Taken together, these observations suggest that GUCY2C-targeted CAR-T cells could eradicate tumors without autoimmunity in patients with metastatic colorectal cancer.

One key limitation to translating ACT to epithelial tumors generally, and colorectal cancer specifically, is the paucity of tumor-specific antigens to which immune cells can be targeted. In that context, targeting tumor-associated self-antigens risks development of "on-target, off-tumor" toxicities and therapy-limiting autoimmunity.[35,36] CEA is an antigen that is normally expressed by intestinal and lung epithelial cells, and overexpressed by colorectal tumors. While T cells directed to CEA exhibit antitumor efficacy, their administration to patients produced treatment-limiting colitis.[8] Similarly, Her-2 also is expressed by normal epithelial cells and overexpressed by colorectal tumors, and T cells targeting this antigen produced lethal immune-mediated damage to normal lung in a patient.[7] In contrast, GUCY2C may be uniquely suited to direct immune cells to colorectal metastases without autoimmunity due to its sequestered expression on apical surfaces of intestinal epithelia.[19-21] Thus, GUCY2C-targeted CAR T cells eradicated GUCY2C-expressing pulmonary metastases without immune damage to intestinal epithelia (Fig. 6). GUCY2C-targeted imaging agents,[23] immunotoxins,[25] and vaccines[26-28] recognize GUCY2C-expressing metastatic colorectal tumors, but not normal intestinal epithelia. Indeed, universal overexpression of GUCY2C on the surface of metastatic tumors,[17,18,37] but its absence on basolateral membranes of epithelial cells[19-21] may shield normal intestine from systemic GUCY2C-targeted therapies. In that context, T cells directed to CEA, whose epitopes are presented by MHC in apical and basolateral membranes of intestinal cells, were characterized by antigen-dependent intestinal accumulation and colitis in mouse models[38,39] and patients.[8] In contrast, mice treated with GUCY2C CAR-T cells were free of intestinal accumulation and toxicity (Fig. 6), underscoring the importance of GUCY2C sequestration in apical membranes to prevent CAR-T cell recognition, accumulation, and toxicity. Beyond intestinal mucosa, GUCY2C expression recently was described in neurons of hypothalamus,
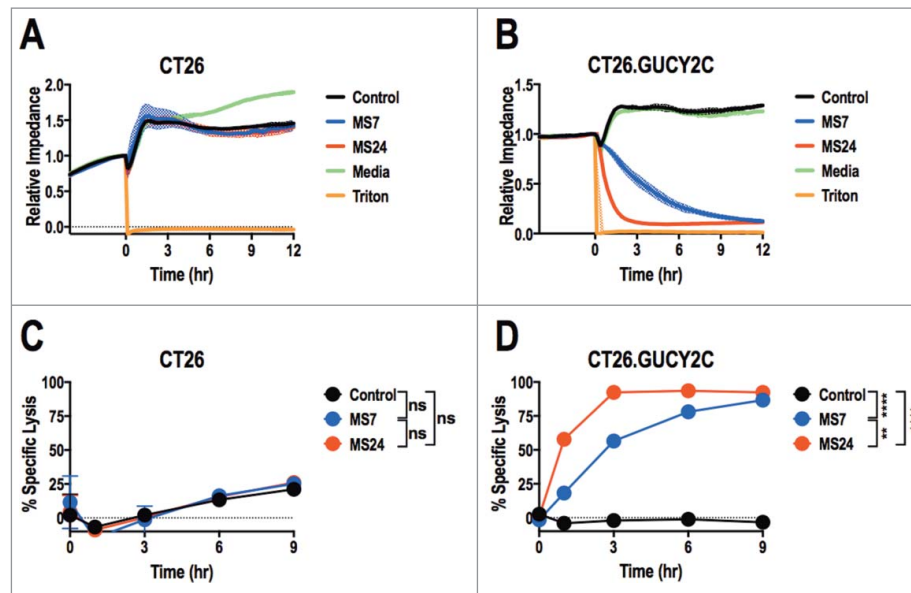
Figure 4. Real-time GUCY2C-specific CAR T cell-mediated cytotoxicity. CT26 (A and C) or CT26.GUCY2C (B and D) mouse colorectal cancer cells were seeded at 10,000 cells/well in an E-Plate and CAR-T cells, media, or Triton-X 100 (Triton) were added to the plate 24 h later (time = 0). The E-Plate was scanned every 15 min to quantify relative electrical impedance (normalized to time = 0). (A and B) Solid lines indicate the mean of duplicate wells and surrounding clouds indicate standard deviation. Results are representative of two experiments. (C and D) % specific lysis values for each CAR-T cell and target cell combination were calculated from the impedance data at the indicated time points. All statistical tests in (C) and (D) compared (1) Control to MS7, (2) Control to MS24, and (3) MS7 to MS24 (**$p < 0.01$, ****$p < 0.0001$, Two-way ANOVA). (C and D) show the means ± standard deviation of two experiments.

an immunologically privileged compartment, where it regulates satiety and appetite.[40] GUCY2C levels in hypothalamus are 10-fold lower than those in intestine.[40] In that context, sufficient quantities of antigen on the surface of cellular targets are necessary to induce CAR T cell activation.[41] GUCY2C-targeted CAR T cells or immunotoxins[25] did not damage hypothalamic neurons, supporting the suggestion that they are sequestered from systemically targeted agents and/or express GUCY2C at levels below detection by our monoclonal antibodies. Taken together, the narrow pattern of expression in normal tissues, expression in compartments which are anatomically shielded or immunologically privileged, and universal overexpression by metastatic tumors suggest that GUCY2C is uniquely qualified as an antigenic target to which T cells can be directed to treat metastatic CRC without autoimmunity.

Beyond selectivity of expression in normal tissues and tumors, aligning ACT platforms with patterns of antigen expression within tissues can minimize treatment-limiting adverse events. For example, CEA is expressed in apical membranes of intestinal epithelial cells, and is presumably inaccessible to targeted CAR-T cells which recognize native antigen in an MHC-independent fashion.[5,42] Indeed, CAR-T cells directed to human CEA did not produce colitis in a transgenic mouse model recapitulating human CEA expression.[38] However, T cells directed by recombinant TCRs recognize peptide antigens in the context of MHC.[43] In turn, MHC-peptide complexes can be presented on basolateral membranes of intestinal epithelial cells[44] or cross-presented by antigen-presenting cells in tissues or lymphoid organs,[45] abrogating the anatomical shielding of natively-expressed apical membrane proteins. Indeed, T cells directed by CEA-specific TCRs produce severe colitis in mice and humans.[8,39] Thus, aligning GUCY2C as an apical target antigen, with CAR platforms to direct MHC-independent elimination of tumor cells, should maximize the

benefit of luminal sequestration in normal tissues, optimizing therapeutic discrimination between tumors and intestine, as observed here.

Utilization of receptors targeting self-antigens to direct engineered T cells, and the associated incomplete discrimination of normal tissues and tumors, creates an imperative to define their safety and therapeutic efficacy in preclinical models that emulate the expression of target antigens in patients. However, the translation of ACT to patient-based trials has been based largely on the safety and efficacy of these paradigms in artificial human tumor xenograft systems. In some cases, the target antigen was not expressed in normal tissues, making it impossible to assess safety.[9,10] In other cases, transgenic models attempt to emulate the expression of the human antigen in normal tissues in patients. For example, CEA CAR-T cells exhibited antitumor efficacy without immune-mediated damage to normal tissues in CEA-transgenic mice.[38] Nevertheless, safety profiles achieved with artificial xenogeneic preclinical models must be viewed with some caution. Indeed, in other CEA transgenic mouse models, antitumor efficacy of CEA-specific T cells was associated with severe immune-mediated colitis.[39] More significantly, a recent clinical trial of CEA-specific T cells induced severe autoimmune colitis, which represented dose-limiting toxicity and required discontinuation of therapy.[8] Further, human Her-2 transgenic mice treated with large doses of CAR-T cells derived from the human Her-2 specific antibody 4D5,[46] but not the FRP5 antibody,[47] caused death within 4 d of treatment. This effect was not achieved with lower doses of 4D5 CAR-T cells; however, a colorectal cancer patient treated with 4D5 CAR-T cells also died following treatment, with potential evidence of antigen-specific toxicities in lung epithelium.[7] These conflicting reports highlight the challenges of extrapolating safety profiles of ACT defined in transgenic mouse models, particularly if antigen expression levels do not mimic those in humans.
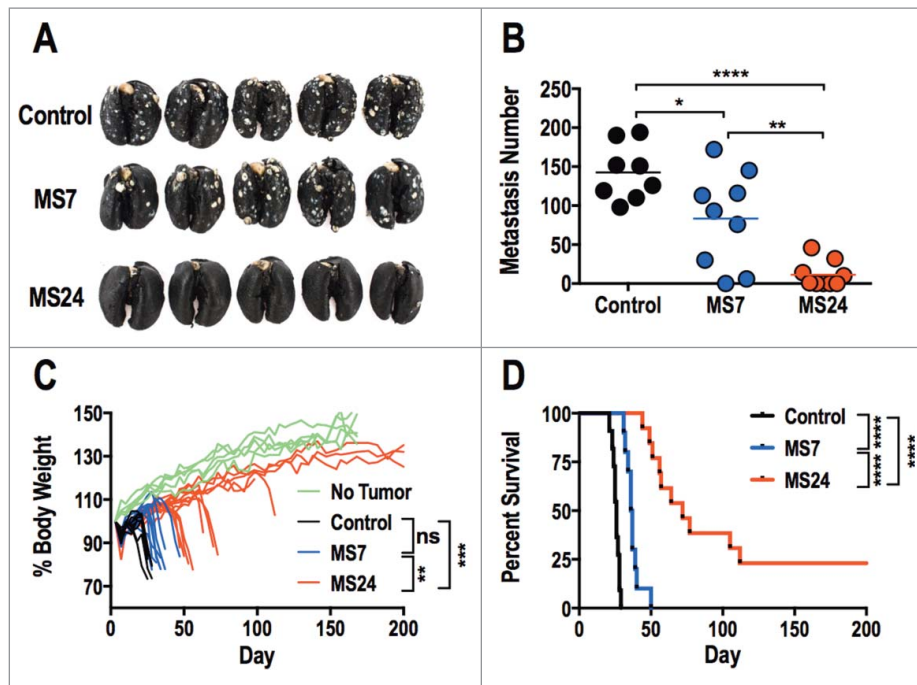
Figure 5. GUCY2C-specific CAR T cells oppose parenchymal colorectal cancer metastases. (A–D) BALB/c mice were injected i.v. with 5×10^5 CT26.GUCY2C cells to establish lung metastases. On day 3, mice received a dose of 5 Gy TBI followed by an i.v. injection of 1×10^7 CAR-T cells. Mice were sacrificed on day 24 after tumor inoculation, lungs were stained with India ink, and tumor nodules were counted (A and B), or mice were followed longitudinally for morbidity (C) and survival (D). (A) Representative images of lungs collected and stained on day 24. (B) Quantification of metastases in each mouse. (N = 8–9 mice/group; $^*p < 0.05$, $^{**}p < 0.01$, and $^{****}p < 0.0001$, One-way ANOVA). (C) Body weight curves of mice relative to initial body weight indicating progression of cancer cachexia, where each line represents an individual mouse. No Tumor represents curves of unmanipulated mice. (n = 10–13 mice/group; ns = not significant, $^{**} p < 0.01$, $^{***} p < 0.001$, One-way ANOVA of total area under the curve). (D) Survival analysis (n = 10–13 mice/group; $^{****}p < 0.0001$, Mantel-Cox log-rank test). All statistical tests in (B–D) compared (1) Control to MS7, (2) Control to MS24, and (3) MS7 to MS24.

These considerations underscore the importance of establishing safety and efficacy profiles of ACT in syngeneic models in which engineered T cells are directed by receptors targeting antigens endogenously expressed in normal tissues.[11] Indeed, CAR-T cells targeting murine CD19 eliminate B cell leukemia in mice with concomitant loss of normal B cells,[12,48] recapitulating observations in clinical trials.[4,5] Separately CAR-T cells targeting stromal FAP and VEGFR-2 also produce significant toxicities in mice.[13,49] CAR-T cells targeting FAP cause lethal bone marrow toxicity in mice reflecting FAP expression on multipotent bone marrow stem cells.[13] Further, VEGFR-2 CAR-T cells caused toxicity only in tumor-bearing mice, mediated by CAR-expressing CD4$^+$, but not CD8$^+$, T cells.[49] In the present study, we demonstrated that CAR-T cells directed to murine GUCY2C eradicated GUCY2C-expressing colorectal tumors metastatic to lungs, without inducing autoimmunity in intestine or other normal tissues in mice endogenously expressing the target antigen. However, CAR-T cell toxicity typically reflects acute cytokine production and tissue damage,[50] and the long-term toxicity of GUCY2C CAR-T cell therapy could not be evaluated here. In that context, GUCY2C CAR-T cell persistence was limited (Fig. S6), reflecting their production in the presence of IL-2. Recent analysis of the impact of cytokine milieu during CAR-T cell production and *in vivo* following their administration, suggest that alternative cytokine combinations may produce CAR-T cells with enhanced persistence and antitumor efficacy.[51] Indeed, CAR-T cell production in the presence of IL-2 produced highly differentiated CAR-T cells with the least *in vivo* persistence and antitumor efficacy,

compared to IL-7, IL-15, IL-18, IL-21, or no cytokines. Thus, as cell production methods continue to be refined, toxicity will be re-evaluated to determine if improving GUCY2C CAR-T cell persistence and antitumor efficacy concomitantly increases their associated toxicity targeting antigen-expressing tissues.

Taken together, these observations provide proof-of-principle in a uniquely relevant preclinical syngeneic model that GUCY2C-targeted CAR-T cells could be clinically effective, without inducing autoimmune tissue damage, in patients with metastatic colorectal cancer. This paradigm leverages the unique structural compartmentalization of GUCY2C endogenously expressed in normal tissues,[19-22] and the universal overexpression of this antigen by metastatic colorectal tumors.[17,18,37] It offers an immunotherapeutic strategy to treat bulky metastatic disease, which is complementary to GUCY2C vaccines as secondary prevention of metastatic disease in CRC patients at risk.[26-28] The significance of these observations can best be appreciated by considering that metastatic CRC is nearly always fatal, without curative therapeutic options.[1] Moreover, beyond CRC, GUCY2C-targeted ACT offers a unique therapeutic option to treat metastases in patients with gastric, esophageal, and pancreatic cancers which also are universally fatal and which ectopically express GUCY2C after transformation.[17] Translation of these observations into patients will require the development of monoclonal antibodies to human GUCY2C, their incorporation into CAR constructs, and testing of their therapeutic efficacy in mice harboring human colorectal cancer metastases.

Materials and methods

Mouse GUCY2C monoclonal antibodies

The monoclonal antibodies (MS7, MS20, and MS24) recognize mouse GUCY2C,[40] CT26.GUCY2C cells,[28] and 6xHis-tagged GUCY2C$_{ECD}$ protein.[28] GUCY2C-specific antibodies were tested by ELISA as previously described.[28] *FACS*: CT26 tumor cells were stained with 10 μg/mL GUCY2C-specific antibody follow by detection with anti-mouse conjugated to Alexa-488 and assessed for surface expression using the BD LSR II flow cytometer. *Immunohistochemistry*: intestinal tissues from wild-type and *Gucy2c*$^{-/-}$ BALB/c mice were fixed in formalin and paraffin embedded. Tissue sections were stained with 5 μg/mL GUCY2C-specific monoclonal antibody followed by detection with anti-mouse antibody conjugated to Alexa-488 and mounted in ProLong Gold Antifade Reagent with DAPI (Life Technologies). Images were captured using the EVOS FL Auto Cell imaging system.

CAR construction

A third generation codon-optimized CAR was synthesized containing the BiP (GRP-78) signal peptide, and scFv from the murine 4D5 monoclonal antibody specific for human ERBB2,[52] CD8α hinge region, CD28 transmembrane and intracellular domains, and 4-1BB (CD137) and CD3ζ intracellular domains in the pMA entry plasmid (GeneArt). CARs derived from the 4D5 antibody served as the negative control CAR in all experiments performed. V$_L$ and V$_H$ variable regions were cloned from MS7, MS20, and MS24 hybridomas by RT-PCR using degenerate primers and linked with a glycine-serine linker (G$_4$S)$_4$ by overlap extension PCR. Resulting GUCY2C-specific scFv constructs were subcloned into the synthesized CAR construct, replacing 4D5.

Retrovirus production and T cell transduction

CARs were subcloned into the pMSCV-IRES-GFP (pMIG) retroviral vector using XhoI and EcoRI restriction sites. The Phoenix-Eco retroviral packaging cell line (Gary Nolan, Stanford University) was transfected with CAR-pMIG vectors and the pCL-Eco retroviral packaging vector (Imgenex) using the Calcium Phosphate Profection^R Mammalian Transfection System (Promega). Retrovirus-containing supernatants were collected 48 h later, filtered through 0.45 μM filters, and aliquots were frozen at −80°C. Murine CD8$^+$ T cells were purified from BALB/c splenocytes using the CD8α+ T cell Isolation Kit II (Miltenyi Biotec) and subsequently stimulated with αCD3/αCD28-coated beads (T Cell Activation/Expansion Kit, Miltenyi Biotec) at a 1:1 bead:cell ratio at 1 × 10^6 cells/mL in cRPMI (RMPI + 10% FBS, 10 μM HEPES, 0.05 μM 2-mercaptoethanol) with 100 U/mL recombinant human IL-2 (NCI Repository). The day following stimulation, $\frac{1}{2}$ of the culture media was carefully replaced with an equal volume of thawed retroviral supernatant in the presence of polybrene (Millipore). Spinoculation was performed at room temperature for 90 min at 2,500 rpm followed by incubation at 37°C for 2.5 h at which point cells were pelleted and resuspended in fresh media containing IL-2. T cells were expanded for 7–10 d by daily dilution to 1 × 10^6 cells/mL with fresh cRPMI and IL-2 at which point they were used for functional assays. All cell counts employed a Muse Cell Analyzer and Count and Viability Assay (Millipore). Serum lots were not pretested for performance.

CAR surface detection

CAR-transduced T cells were stained with the Live/Dead Fixable Aqua Dead Cell Stain kit (Invitrogen), labeled with varying concentrations of 6xHis-tagged GUCY2C$_{ECD}$ for 1 h, stained with the α5xHis Alexa-647 conjugate (Qiagen) and αCD8b-PE (clone H35.17.2, BD Biosciences) for 1 h, fixed with 2% PFA and analyzed using the BD LSR II flow cytometer and FlowJo software (Tree Star). GUCY2C binding was quantified by determining the mean fluorescence intensity of Alexa-647 on live CD8$^+$ GFP$^+$ cells. Non-linear regression analysis (GraphPad Prism v6) was used to determine the K$_{av}$ and B$_{max}$ of GUCY2C-CAR binding.

Surface activation marker and intracellular cytokine staining

CAR-transduced T cells were stimulated for 6 h with antigen coated on tissue culture plates at 1 μg/mL in PBS overnight at 4°C, or with Cell Stimulation Cocktail (PMA/Ionomycin, eBioscience). Incubation included the Protein Transport Inhibitor Cocktail (eBioscience) when assessing intracellular cytokines. Cells were stained with Live/Dead fixable Aqua Dead Cell stain kit (Invitrogen) and subsequently stained for surface markers using the following antibodies: αCD8α-PerCP-Cy5.5 (clone 53.6-7) and αCD69-PE (clone H1.2F3) from BD Biosciences and αCD25-PE (clone PC61.5, eBioscience). Intracellular cytokine staining was performed using the BD Cytofix/Cytoperm Kit (BD Biosciences) and staining with the following antibodies: αGFP-Alexa-488 (Invitrogen), αIFNγ-APC-Cy7 (XMG1.2) and αTNFα-PE-Cy7 (MP6-XT22) from BD Biosciences, and αMIP1α-PE (clone 39624, R&D Systems). Cells were fixed in 2% PFA and analyzed on a BD LSR II flow cytometer. Analyses were performed using FlowJo software (Tree Star).

Real time cell-mediated cytotoxicity assay

The xCELLigence system (Acea Biosciences Inc.) was utilized for assessment of T cell-mediated cytotoxicity.[53] Briefly 1 × 10^4 CT26 or CT26.GUCY2C targets were plated in 150 μL of DMEM 10% FBS in each well of an E-Plate 16 and grown overnight, quantifying electrical impedance every 15 min, using the RTCA DP Analyzer system (Acea Biosciences Inc.). Approximately 24 h later, 50 μL of CAR-T cells was added at an effector-to-target (E:T) ratio of 5:1 or 50 μL of media or 10% Triton-X 100 were added as negative and positive controls, respectively. Cell-mediated killing was quantified over the next 16 h reading electrical impedance every 15 min. Percent-specific lysis values were calculated using GraphPad Prism Software v6 for each replicate at each time point, using impedance values following the addition of media and Triton for normalization (0% and 100% specific lysis, respectively).
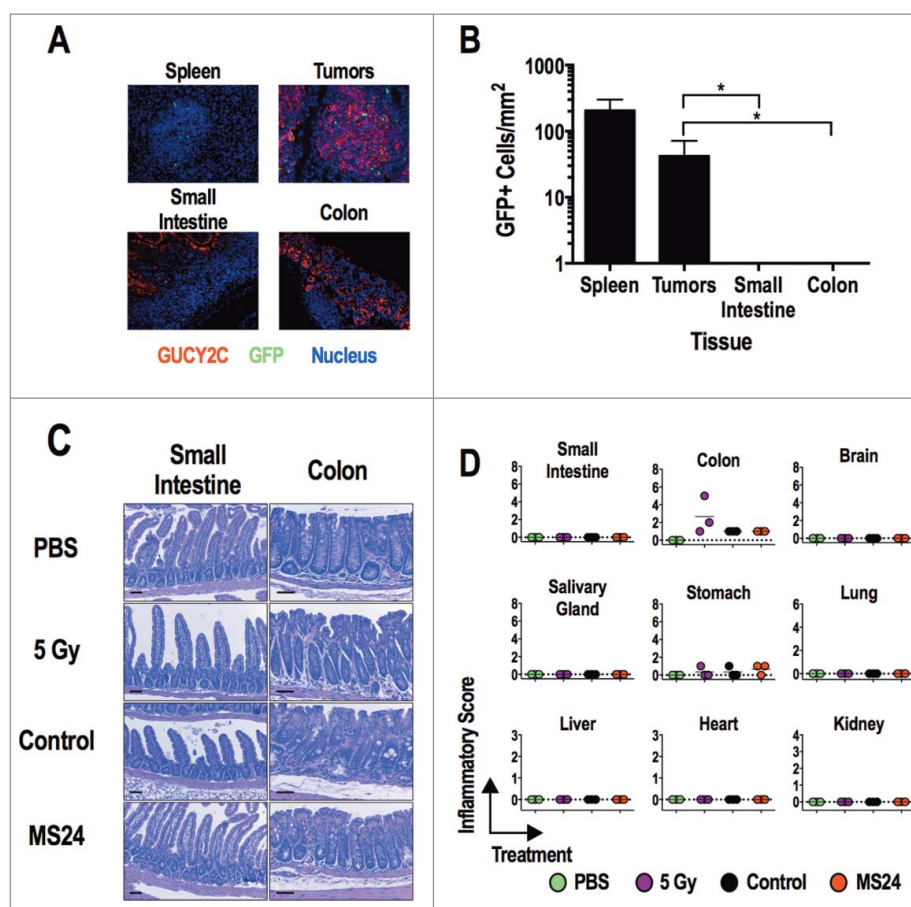
Figure 6. GUCY2C-specific CAR T cells do not induce tissue damage. (A and B) MS24 CAR-T cells were administered to BALB/c mice with CT26.GUCY2C lung metastases established 14 d earlier following 5 Gy TBl. (A) Lungs, spleens, and intestines were collected 2 d later, and tissue sections were stained with anti-GUCY2C (red) and anti-GFP (green) antibodies and counterstained with DAPI. (B) GFP+ MS24 CAR-T cells were quantified in remnant follicles in spleen, tumor metastases in lungs, and Peyer's patches in intestines by immunostaining of GFP. Data represent the mean of four mice. (****$p < 0.001$, One-way ANOVA compared to accumulation in lung metastases). (C and D) BALB/c mice were treated with PBS, 5 Gy TBl, 5 Gy TBl + 1×10^7 Control or MS24 CAR-T cells. On day 6 post-treatment, mice were sacrificed and tissues collected, fixed in formalin, and paraffin embedded. Slides were stained with H&E and scored for pathology. Scale bars indicate 100 μm. (C) Representative H&E-stained small intestine and colon sections. (D) Inflammatory scoring for all tissues collected. No significant differences between Control and MS24 CAR-T cell treatment groups were detected (One-way ANOVA).

Metastatic tumor model

BALB/c mice were obtained from the NCI Animal Production Program (Frederick, MD). Animal protocols were approved by the Thomas Jefferson University Institutional Animal Care and Use Committee. Male BALB/c mice were challenged with 5×10^5 CT26.GUCY2C cells by tail vein injection to establish lung metastases. On day 3 following tumor injections, mice received a non-myeloablative dose of 5 Gy total body irradiation in a PanTak, 310 kVe x-ray machine. Mice received 1×10^7 fresh CAR-T cells in 100 μL PBS following irradiation by tail vein injection. Mice were followed for cachexia (twice weekly body weights) and survival, or sacrificed at day 23 after tumor cell injection and lungs were stained with India ink and fixed in Fekete's solution for tumor enumeration.[28]

Toxicity

For T cell accumulation, 1×10^7 MS24 CAR-T cells were administered to BALB/c mice with CT26.GUCY2C lung metastases established 14 d earlier following 5 Gy TBI. Lungs, spleens, and intestines were collected 2 d later, and

tissue sections were stained with anti-GUCY2C (MS20) and anti-GFP antibodies and counterstained with DAPI. GFP+ MS24 CAR-T cells were quantified in remnant follicles in spleen, tumor metastases in lungs, and Peyer's patches in intestines and normalized to area (mm^2). A cell was considered to be GFP+ if fluorescence intensity was above the background level (set using corresponding GFP-negative control tissues) associated with a DAPI-stained nucleus in the same plane. For histopathology, tissues and serum were collected from mice 6 d after treatment with PBS, 5 Gy TBI, or 5 Gy TBI and CAR-T cells. Tissues were fixed in formalin and embedded in paraffin. Sections were stained with hematoxylin and eosin and scored for toxicity by a blinded pathologist (P.L.). Scoring criteria are listed in Table S1. Serum chemistries were commercially determined (Charles River Laboratories).

Statistical analyses

Statistical analyses were conducted using GraphPad Prism Software v6. All results are representative of at least three experiments unless otherwise indicated.

Disclosure of potential conflicts of interest

Funding

ORCID

Adam E. Snook (ID icon) http://orcid.org/0000-0001-9216-4560

References

1. Howlader N, Noone AM, Krapcho M, Garshell J, Miller D, Altekruse SF, Kosary CL, Yu M, Ruhl J, Tatalovich Z,Mariotto A, Lewis DR, Chen HS, Feuer EJ, Cronin KA (eds). SEER Cancer Statistics Review, 1975-2012, National Cancer Institute. Bethesda, MD, http://seer.cancer.gov/csr/1975_2012/, based on November 2014 SEER data submission, posted to the SEER web site, April 2015.

2. Couzin-Frankel J. Breakthrough of the year 2013. Cancer immunotherapy. Science 2013; 342:1432-3; PMID:24357284; http://dx.doi.org/10.1126/science.342.6165.1432

3. Dudley ME, Wunderlich JR, Robbins PF, Yang JC, Hwu P, Schwartzentruber DJ, Topalian SL, Sherry R, Restifo NP, Hubicki AM et al. Cancer regression and autoimmunity in patients after clonal repopulation with antitumor lymphocytes. Science 2002; 298:850-4; PMID:12242449; http://dx.doi.org/10.1126/science.1076514

4. Grupp SA, Kalos M, Barrett D, Aplenc R, Porter DL, Rheingold SR, Teachey DT, Chew A, Hauck B, Wright JF et al. Chimeric antigen receptor-modified T cells for acute lymphoid leukemia. N Engl J Med 2013; 368:1509-18; PMID:23527958; http://dx.doi.org/10.1056/NEJMoa1215134

5. Porter DL, Levine BL, Kalos M, Bagg A, June CH. Chimeric antigen receptor-modified T cells in chronic lymphoid leukemia. N Engl J Med 2011; 365:725-33; PMID:21830940; http://dx.doi.org/10.1056/NEJMoa1103849

6. Louis CU, Savoldo B, Dotti G, Pule M, Yvon E, Myers GD, Rossig C, Russell HV, Diouf O, Liu E et al. Antitumor activity and long-term fate of chimeric antigen receptor-positive T cells in patients with neuroblastoma. Blood 2011; 118:6050-6; PMID:21984804; http://dx.doi.org/10.1182/blood-2011-05-354449

7. Morgan RA, Yang JC, Kitano M, Dudley ME, Laurencot CM, Rosenberg SA. Case report of a serious adverse event following the administration of T cells transduced with a chimeric antigen receptor recognizing ERBB2. Mol Ther 2010; 18:843-51; PMID:20179677; http://dx.doi.org/10.1038/mt.2010.24

8. Parkhurst MR, Yang JC, Langan RC, Dudley ME, Nathan DA, Feldman SA, Davis JL, Morgan RA, Merino MJ, Sherry RM et al. T cells targeting carcinoembryonic antigen can mediate regression of metastatic colorectal cancer but induce severe transient colitis. Mol Ther 2011; 19:620-6; PMID:21157437; http://dx.doi.org/10.1038/mt.2010.272

9. Zhao Y, Wang QJ, Yang S, Kochenderfer JN, Zheng Z, Zhong X, Sadelain M, Eshhar Z, Rosenberg SA, Morgan RA. A herceptin-based chimeric antigen receptor with modified signaling domains leads to enhanced survival of transduced T lymphocytes and antitumor activity. J Immunol 2009; 183:5563-74; PMID:19843940; http://dx.doi.org/10.4049/jimmunol.0900447

10. Parkhurst MR, Joo J, Riley JP, Yu Z, Li Y, Robbins PF, Rosenberg SA. Characterization of genetically modified T-cell receptors that recognize the CEA:691-699 peptide in the context of HLA-A2.1 on human colorectal cancer cells. Clin Cancer Res 2009; 15:169-80; PMID:19118044; http://dx.doi.org/10.1158/1078-0432.CCR-08-1638

11. Sampson JH, Choi BD, Sanchez-Perez L, Suryadevara CM, Snyder DJ, Flores CT, Schmittling RJ, Nair SK, Reap EA, Norberg PK et al. EGFRvIII mCAR-modified T-Cell therapy cures mice with established intracerebral glioma and generates host immunity against Tumor-Antigen loss. Clin Cancer Res 2014; 20:972-84; PMID:24352643; http://dx.doi.org/10.1158/1078-0432.CCR-13-0709

12. Kochenderfer JN, Yu Z, Frasheri D, Restifo NP, Rosenberg SA. Adoptive transfer of syngeneic T cells transduced with a chimeric antigen receptor that recognizes murine CD19 can eradicate lymphoma and normal B cells. Blood 2010; 116:3875-86; PMID:20631379; http://dx.doi.org/10.1182/blood-2010-01-265041

13. Tran E, Chinnasamy D, Yu Z, Morgan RA, Lee CC, Restifo NP, Rosenberg SA. Immune targeting of fibroblast activation protein triggers recognition of multipotent bone marrow stromal cells and cachexia. J Exp Med 2013; 210:1125-35; PMID:23712432; http://dx.doi.org/10.1084/jem.20130110

14. Frick GS, Pitari GM, Weinberg DS, Hyslop T, Schulz S, Waldman SA. Guanylyl cyclase C: a molecular marker for staging and postoperative surveillance of patients with colorectal cancer. Expert Rev Mol Diagn 2005; 5:701-13; PMID:16149873; http://dx.doi.org/10.1586/14737159.5.5.701

15. Carrithers SL, Barber MT, Biswas S, Parkinson SJ, Park PK, Goldstein SD, Waldman SA. Guanylyl cyclase C is a selective marker for metastatic colorectal tumors in human extraintestinal tissues. Proc Natl Acad Sci U S A 1996; 93:14827-32; PMID:8962140; http://dx.doi.org/10.1073/pnas.93.25.14827

16. Snook AE, Eisenlohr LC, Rothstein JL, Waldman SA. Cancer mucosa antigens as a novel immunotherapeutic class of tumor-associated antigen. Clin Pharmacol Ther 2007; 82:734-9; PMID:17898707; http://dx.doi.org/10.1038/sj.clpt.6100369

17. Birbe R, Palazzo JP, Walters R, Weinberg D, Schulz S, Waldman SA. Guanylyl cyclase C is a marker of intestinal metaplasia, dysplasia, and adenocarcinoma of the gastrointestinal tract. Hum Pathol 2005; 36:170-9; PMID:15754294; http://dx.doi.org/10.1016/j.humpath.2004.12.002

18. Schulz S, Hyslop T, Haaf J, Bonaccorso C, Nielsen K, Witek ME, Birbe R, Palazzo J, Weinberg D, Waldman SA. A validated quantitative assay to detect occult micrometastases by reverse transcriptase-polymerase chain reaction of guanylyl cyclase C in patients with colorectal cancer. Clin Cancer Res 2006; 12:4545-52; PMID:16899600; http://dx.doi.org/10.1158/1078-0432.CCR-06-0865

19. Charney AN, Egnor RW, Alexander-Chacko JT, Zaharia V, Mann EA, Giannella RA. Effect of E. coli heat-stable enterotoxin on colonic transport in guanylyl cyclase C receptor-deficient mice. Am J Physiol Gastrointest Liver Physiol 2001; 280:G216-21; PMID:11208543

20. Kuhn M, Adermann K, Jahne J, Forssmann WG, Rechkemmer G. Segmental differences in the effects of guanylin and Escherichia coli heat-stable enterotoxin on Cl⁻ secretion in human gut. J Physiol 1994; 479(Pt 3):433-40; PMID:7837099; http://dx.doi.org/10.1113/jphysiol.1994.sp02-0307

21. Guarino A, Cohen MB, Overmann G, Thompson MR, Giannella RA. Binding of E. coli heat-stable enterotoxin to rat intestinal brush borders and to basolateral membranes. Dig Dis Sci 1987; 32:1017-26; PMID:3304888; http://dx.doi.org/10.1007/BF01297193

22. Hodson CA, Ambrogi IG, Scott RO, Mohler PJ, Milgram SL. Polarized apical sorting of guanylyl cyclase C is specified by a cytosolic signal. Traffic 2006; 7:456-64; PMID:16536743; http://dx.doi.org/10.1111/j.1600-0854.2006.00398.x

23. Wolfe HR, Mendizabal M, Lleong E, Cuthbertson A, Desai V, Pullan S, Fujii DK, Morrison M, Pither R, Waldman SA. In vivo imaging of human colon cancer xenografts in immunodeficient mice using a guanylyl cyclase C-specific ligand. J Nucl Med 2002; 43:392-9; PMID:11884500

24. Almhanna K, Kalebic T, Cruz C, Faris JE, Ryan DP, Jung JA, Wyant T, Fasanmade A, Messersmith WA, Rodon J. Phase I study of the investigational anti-guanylyl cyclase antibody-drug conjugate TAK-264 (MLN0264) in adult patients with advanced gastrointestinal malignancies. Clin Cancer Res 2016; PMID:27178743; http://dx.doi.org/10.1158/1078-0432.ccr-15-2474

25. Marszalowicz GP, Snook AE, Magee MS, Merlino D, Bertman-Booty LD, Waldman SA. GUCY2C lysosomotropic endocytosis delivers immunotoxin therapy to metastatic colorectal cancer. OncoTarget 2014; 5:9460-71; PMID:25294806; http://dx.doi.org/10.18632/oncotarget.2455

26. Snook AE, Magee MS, Schulz S, Waldman SA. Selective antigen-specific CD4(+) T-cell, but not CD8(+) T- or B-cell, tolerance corrupts cancer immunotherapy. Eur J Immunol 2014; 44:1956-66; PMID:24771148; http://dx.doi.org/10.1002/eji.201444539

27. Snook AE, Li P, Stafford BJ, Faul EJ, Huang L, Birbe RC, Bombonati A, Schulz S, Schnell MJ, Eisenlohr LC et al. Lineage-specific T-cell responses to cancer mucosa antigen oppose systemic metastases without mucosal inflammatory disease. Cancer Res 2009; 69:3537-44; PMID:19351847; http://dx.doi.org/10.1158/0008-5472.CAN-08-3386

28. Snook AE, Stafford BJ, Li P, Tan G, Huang L, Birbe R, Schulz S, Schnell MJ, Thakur M, Rothstein JL et al. Guanylyl cyclase C-induced immunotherapeutic responses opposing tumor metastases without autoimmunity. J Natl Cancer Inst 2008; 100:950-61; PMID:18577748; http://dx.doi.org/10.1093/jnci/djn178

29. Robinson E, Bartal A, Mekori T. Results of postoperative treatment of colorectal cancer by radiotherapy, chemotherapy and immunotherapy. Recent Results Cancer Res 1980; 75:80-7; PMID:7232842; http://dx.doi.org/10.1007/978-3-642-81491-4_13

30. Caruso A, Licenziati S, Corulli M, Canaris AD, De Francesco MA, Fiorentini S, Peroni L, Fallacara F, Dima F, Balsari A et al. Flow cytometric analysis of activation markers on stimulated T cells and their correlation with cell proliferation. Cytometry 1997; 27:71-6; PMID:9000587; http://dx.doi.org/10.1002/(SICI)1097-0320(19970101)27:1%3c71::AID-CYT-O9%3e3.0.CO;2-O

31. Mule JJ, Shu S, Schwarz SL, Rosenberg SA. Adoptive immunotherapy of established pulmonary metastases with LAK cells and recombinant interleukin-2. Science 1984; 225:1487-9; PMID:6332379; http://dx.doi.org/10.1126/science.6332379

32. Chamberlain RS, Carroll MW, Bronte V, Hwu P, Warren S, Yang JC, Nishimura M, Moss B, Rosenberg SA, Restifo NP. Costimulation enhances the active immunotherapy effect of recombinant anticancer vaccines. Cancer Res 1996; 56:2832-6; PMID:8665522

33. Gattinoni L, Finkelstein SE, Klebanoff CA, Antony PA, Palmer DC, Spiess PJ, Hwang LN, Yu Z, Wrzesinski C, Heimann DM et al. Removal of homeostatic cytokine sinks by lymphodepletion enhances the efficacy of adoptively transferred tumor-specific CD8+ T cells. J Exp Med 2005; 202:907-12; PMID:16203864; http://dx.doi.org/10.1084/jem.20050732

34. Rosenberg SA, Yang JC, Sherry RM, Kammula US, Hughes MS, Phan GQ, Citrin DE, Restifo NP, Robbins PF, Wunderlich JR et al. Durable complete responses in heavily pretreated patients with metastatic melanoma using T-cell transfer immunotherapy. Clin Cancer Res 2011; 17:4550-7; PMID:21498393; http://dx.doi.org/10.1158/1078-0432.CCR-11-0116

35. Hinrichs CS, Restifo NP. Reassessing target antigens for adoptive T-cell therapy. Nat Biotechnol 2013; 31:999-1008; PMID:24142051; http://dx.doi.org/10.1038/nbt.2725

36. Stauss HJ, Morris EC. Immunotherapy with gene-modified T cells: limiting side effects provides new challenges. Gene Ther 2013; 20:1029-32; PMID:23804078; http://dx.doi.org/10.1038/gt.2013.34

37. Witek ME, Nielsen K, Walters R, Hyslop T, Palazzo J, Schulz S, Waldman SA. The putative tumor suppressor Cdx2 is overexpressed by human colorectal adenocarcinomas. Clin Cancer Res 2005; 11:8549-56; PMID:16361536; http://dx.doi.org/10.1158/1078-0432.CCR-05-1624

38. Chmielewski M, Hahn O, Rappl G, Nowak M, Schmidt-Wolf IH, Hombach AA, Abken H. T cells that target carcinoembryonic antigen eradicate orthotopic pancreatic carcinomas without inducing autoimmune colitis in mice. Gastroenterology 2012; 143:1095-107 e2; PMID:22750462; http://dx.doi.org/10.1053/j.gastro.2012.06.037

39. Bos R, van Duikeren S, Morreau H, Franken K, Schumacher TN, Haanen JB, van der Burg SH, Melief CJ, Offringa R. Balancing between antitumor efficacy and autoimmune pathology in T-cell-mediated targeting of carcinoembryonic antigen. Cancer Res 2008; 68:8446-55; PMID:18922918; http://dx.doi.org/10.1158/0008-5472.CAN-08-1864

40. Valentino MA, Lin JE, Snook AE, Li P, Kim GW, Marszalowicz G, Magee MS, Hyslop T, Schulz S, Waldman SA. A uroguanylin-GUCY2C endocrine axis regulates feeding in mice. J Clin Invest 2011; 121:3578-88; PMID:21865642; http://dx.doi.org/10.1172/JCI57925

41. Chmielewski M, Hombach A, Heuser C, Adams GP, Abken H. T cell activation by antibody-like immunoreceptors: increase in affinity of the single-chain fragment domain above threshold does not increase T cell activation against antigen-positive target cells but decreases selectivity. J Immunol 2004; 173:7647-53; PMID:15585893; http://dx.doi.org/10.4049/jimmunol.173.12.7647

42. Dai H, Wang Y, Lu X, Han W. Chimeric antigen receptors modified T-Cells for cancer therapy. J Natl Cancer Inst 2016; 108; PMID:26819347; https://dx.doi.org/10.1093/jnci/djv439

43. Babbitt BP, Allen PM, Matsueda G, Haber E, Unanue ER. Binding of immunogenic peptides to Ia histocompatibility molecules. Nature 1985; 317:359-61; PMID:3876513; http://dx.doi.org/10.1038/317359a0

44. Bar F, Sina C, Hundorfean G, Pagel R, Lehnert H, Fellermann K, Büning J. Inflammatory bowel diseases influence major histocompatibility complex class I (MHC I) and II compartments in intestinal epithelial cells. Clin Exp Immunol 2013; 172:280-9; PMID:23574324; http://dx.doi.org/10.1111/cei.12047

45. Yu P, Spiotto MT, Lee Y, Schreiber H, Fu YX. Complementary role of CD4+ T cells and secondary lymphoid tissues for cross-presentation of tumor antigen to CD8+ T cells. J Exp Med 2003; 197:985-95; PMID:12695490; http://dx.doi.org/10.1084/jem.20021804

46. Globerson-Levin A, Waks T, Eshhar Z. Elimination of progressive mammary cancer by repeated administrations of chimeric antigen receptor-modified T cells. Mol Ther 2014; 22:1029-38; PMID:24572294; http://dx.doi.org/10.1038/mt.2014.28

47. Wang LX, Westwood JA, Moeller M, Duong CP, Wei WZ, Malaterre J, Trapani JA, Neeson P, Smyth MJ, Kershaw MH et al. Tumor ablation by gene-modified T cells in the absence of autoimmunity. Cancer Res 2010; 70:9591-8; PMID:21098715; http://dx.doi.org/10.1158/0008-5472.CAN-10-2884

48. Cheadle EJ, Hawkins RE, Batha H, O'Neill AL, Dovedi SJ, Gilham DE. Natural expression of the CD19 antigen impacts the long-term engraftment but not antitumor activity of CD19-specific engineered T cells. J Immunol 2010; 184:1885-96; PMID:20089697; http://dx.doi.org/10.4049/jimmunol.0901440

49. Chinnasamy D, Yu Z, Theoret MR, Zhao Y, Shrimali RK, Morgan RA, Feldman SA, Restifo NP, Rosenberg SA. Gene therapy using genetically modified lymphocytes targeting VEGFR-2 inhibits the growth of vascularized syngenic tumors in mice. J Clin Invest 2010; 120:3953-68; PMID:20978347; http://dx.doi.org/10.1172/JCI43490

50. Stauss HJ, Morris EC. Immunotherapy with gene-modified T cells: limiting side effects provides new challenges. Gene Ther 2013; 20(11):1029-32; PMID:23804078; https://dx.doi.org/10.1038/gt.2013.34

51. Xu XJ, Song DG, Poussin M, Ye Q, Sharma P, Rodriguez-Garcia A, Tang YM, Powell DJ. Multiparameter comparative analysis reveals differential impacts of various cytokines on CART cell phenotype and function ex vivo and in vivo. Oncotarget 2016; https://dx.doi.org/10.18632/oncotarget.10510

52. Carter P, Presta L, Gorman CM, Ridgway JB, Henner D, Wong WL, Rowland AM, Kotts C, Carver ME, Shepard HM. Humanization of an anti-p185HER2 antibody for human cancer therapy. Proc Natl Acad Sci U S A 1992; 89:4285-9; PMID:1350088; http://dx.doi.org/10.1073/pnas.89.10.4285

53. Peper JK, Schuster H, Loffler MW, Schmid-Horch B, Rammensee HG, Stevanovic S. An impedance-based cytotoxicity assay for real-time and label-free assessment of T-cell-mediated killing of adherent cells. J Immunol Methods 2014; 405:192-8; PMID:24486140; http://dx.doi.org/10.1016/j.jim.2014.01.012
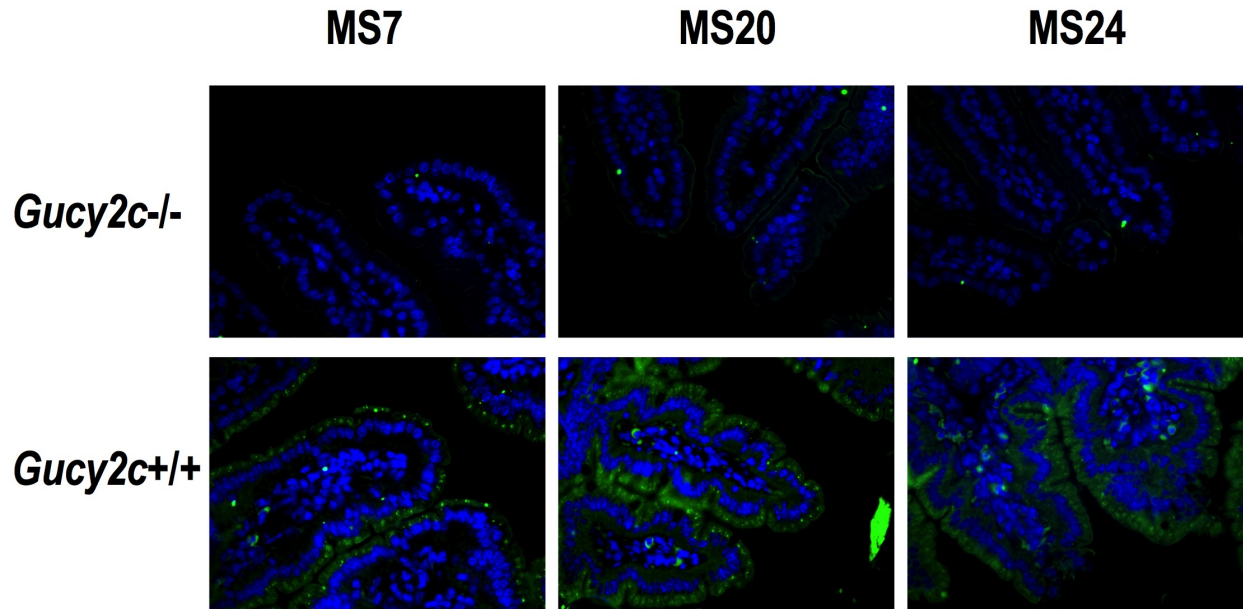
Figure S1. GUCY2C staining in small intestine. Wild-type (*Gucy2c*^{+/+}) or GUCY2C-deficient (*Gucy2c*^{-/-}) mouse small intestine sections were stained with GUCY2C-specific monoclonal antibodies (*green*), demonstrating specificity of antibodies for GUCY2C in the intestine. DAPI (*blue*). Representative of 3 sections each.
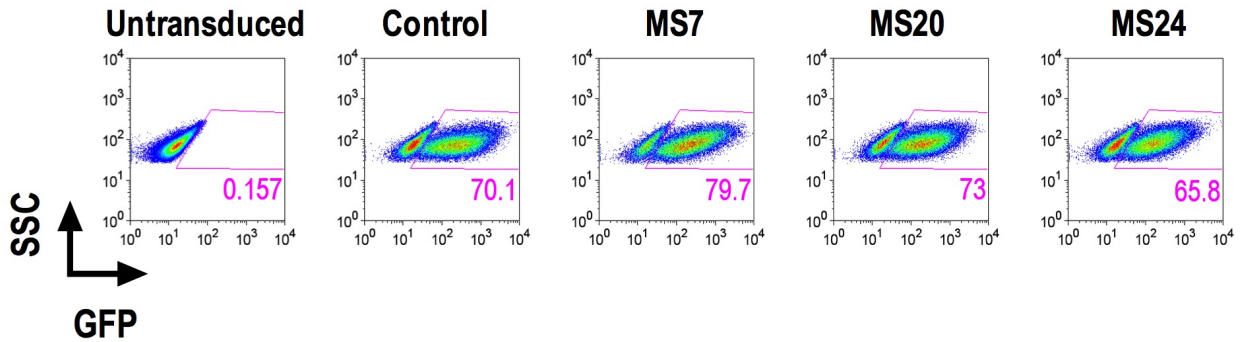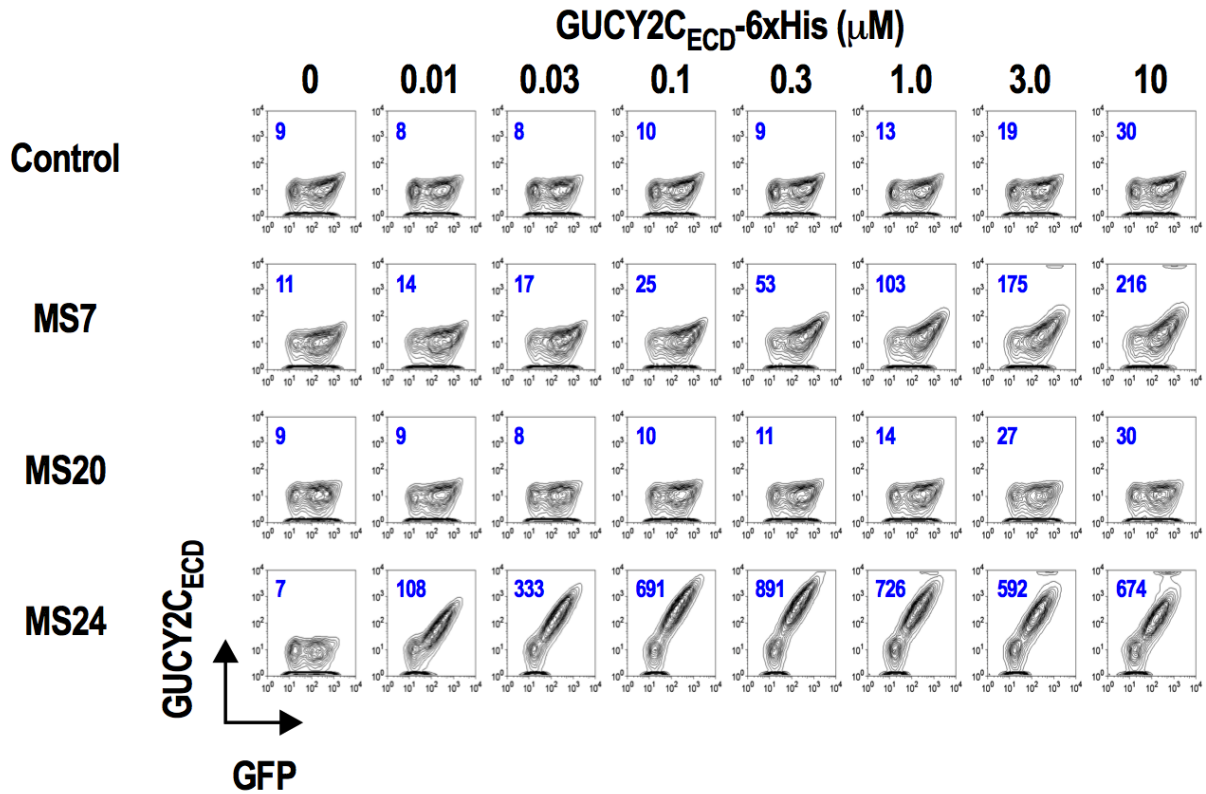
Figure S2. T cell transduction efficiency. Untransduced T cells or T cells transduced with retroviruses containing control, MS7, MS20, or MS24 -derived CARs upstream of an IRES-GFP transduction marker were gated on live CD8^{+} T cells. Magenta numbers indicate the percentage of GFP^{+} T cells.

Supplementary Figure 3

Figure S3. Surface CAR detection. Murine CD8^{+} T cells transduced with a retrovirus containing a Control CAR or CARs derived from GUCY2C antibodies (MS7, MS20 and MS24) were labeled with varying concentrations of purified 6xHis-GUCY2C$_{ECD}$ (0-10 μM) detected with α5xHis-Alexa-647 conjugate. Flow plots were gated on live CD8^{+} cells. Blue numbers indicate the mean fluorescence intensity (MFI) of 6xHis-GUCY2C$_{ECD}$ binding on live CD8^{+} transduced (GFP^{+}) cells. Data are from 3 experiments.
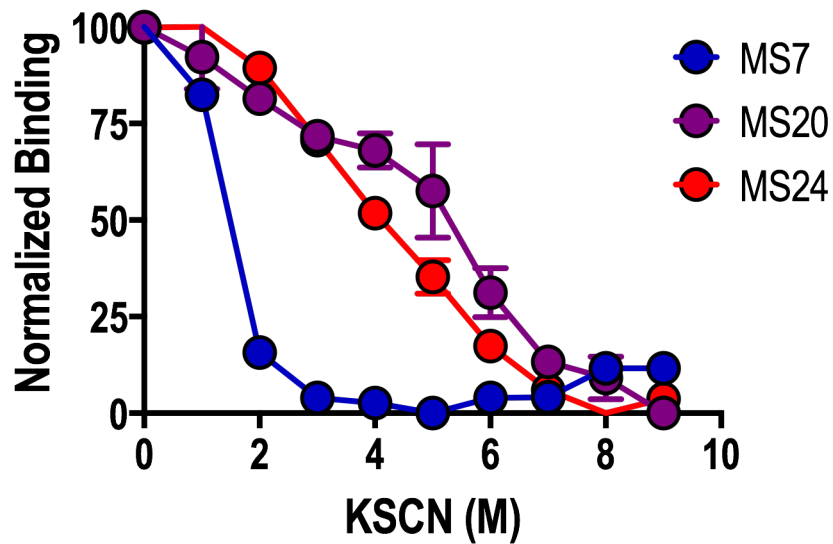
Figure S4. Relative GUCY2C antibody avidities. Relative GUCY2C antibody avidities were determined using a potassium thiocyanate elution ELISA.[1, 2] GUCY2C protein was coated onto ELISA plates and MS7, MS20 and MS24 antibody were then bound to GUCY2C. Wells containing antibody bound to GUCY2C were then exposed to various concentrations of the chaotropic agent potassium thiocyanate (KSCN) and resistance to elution was used as a measure of avidity. MS7 eluted at very low KSCN concentrations, while MS20 and MS24 required high concentrations of KSCN to elute, indicating that MS7 has a substantially lower avidity than MS20 or MS24.
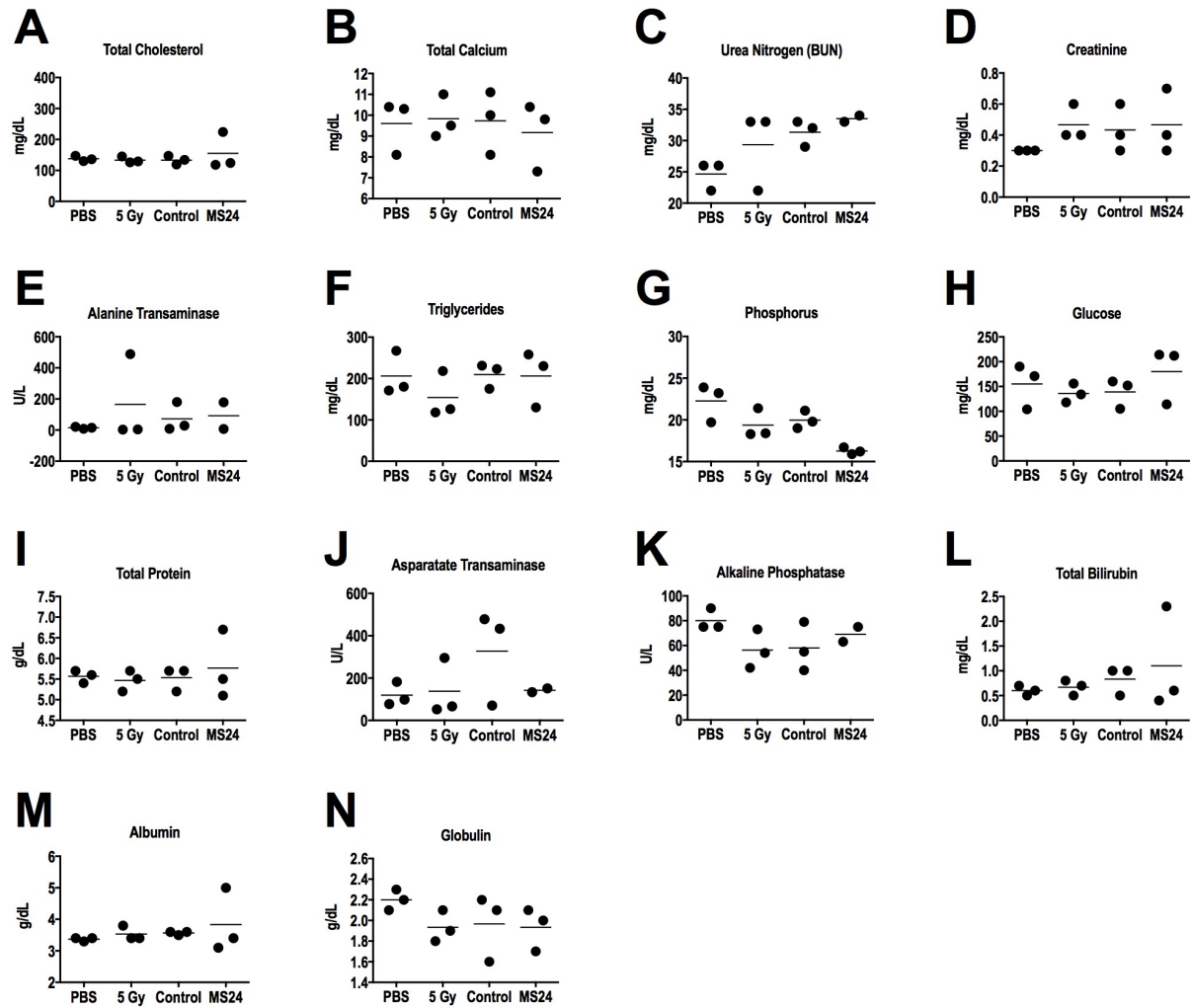
Figure S5. Mouse serum biochemistries following treatment with GUCY2C CAR-T cells. (**A-N**) BALB/c mice were treated with PBS, 5 Gy TBI, 5 Gy TBI + 1x10^7 Control or MS24 CAR-T cells. On day 6 post-treatment, mice were sacrificed, serum collected, and serum chemistry profiles analyzed (Charles River Laboratories). No significant differences between Control and MS24 CAR-T cell treatment groups were detected (One-way ANOVA).
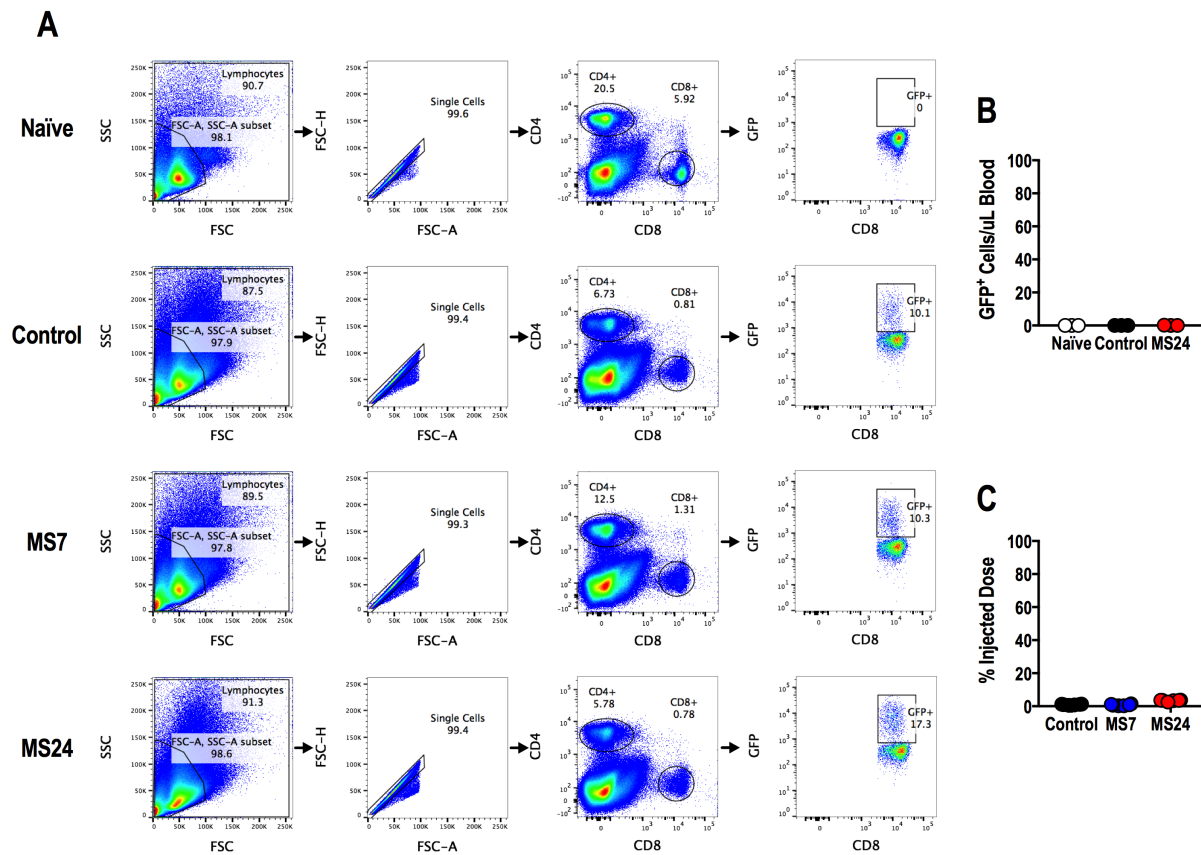
Figure S6. GUCY2C CAR-T cell persistence. (**A-C**) Blood or splenocytes were collected from naïve mice, or mice following CAR-T cell transfer, and stained with αCD4, αCD8, and αGFP. (**A**) Representative splenocyte plots and gating hierarchy 14 days after CAR-T cell transfer, demonstrating that a small number of GFP+ CAR-T cells are detectable. (**B**) Number of live CD8+GFP+ T cells/uL of blood 48 hours after adoptive transfer. No GFP+ CAR-T cells were detectable compared to naïve mice which received no irradiation or CAR-T cell transfer. (**C**) Splenocyte samples collected 14 days after CAR-T cell transfer were analyzed as in **A**. Here, the entire splenocyte population was analyzed to quantify the total number of GFP+ cells/spleen. The % injected dose was then calculated (GFP+ cells/spleen ÷ 3×10^6 GFP+ cells/mouse × 100%).

Table S1. T-cell mediated tissue damage scoring system

Organs	T-cell mediated tissue damage			
Colon and small intestine[3]	Score	Epithelial lesion	Mesenchymal lesion	Total score
	0	Normal	No inflammatory infiltrates	0
	1	Loss of goblet cells	Inflammatory infiltrate around crypt base	2
	2	Loss of goblet cells in large areas	Inflammatory infiltrate reaching muscularis mucosae	4
	3	Loss of crypts	Extensive infiltration reaching the muscularis mucosae, thickening of the mucosa with abundant edema	6
	4	Loss of crypts in large area	Inflammatory infiltration of the submucosa	8
Stomach[4]	0	Normal	No inflammatory infiltrates	0
	1	Single cells apoptosis noted in medium power	Rare inflammatory infiltrates	2
	2	Evidence of epithelial damage by crypt/glandular abscesses, epithelial flattening or glandular dilation	Mild inflammatory infiltrates	4
	3	Dropout of one or more crypts/glands	Moderate inflammatory infiltrates	6
	4	Total epithelial denudation	Confluent inflammatory infiltrates	8
Salivary gland[5]	0	Normal	No inflammatory infiltrates	0
	1	Mild exocytosis of lymphocytes into epithelium salivary gland	Mild interstitial inflammation	2
	2	Exocytosis of lymphocytes, mild acinar destruction, ductal dilatation, squamous metaplasia, mucous pooling, duct cell proliferation	Moderately intense band of lymphocytes in submucosa, mild fibrosis	4
	3	Exocytosis of lymphocytes into epithelial salivary gland, diffuse destruction of ducts and acini	Heavy submucosal band of lymphocytes, marked interstitial lymphocytic infiltrates	6
	4	Nearly complete loss of acini, marked dilated ducts	Interstitial fibrosis with or without inflammation	8
Lung[6]	Score	Vessels	Small airways	Total score
	0	No evidence of mononuclear cell infiltration, hemorrhage or necrosis	No evidence of bronchiolar inflammation	0
	1	Scattered, infrequent perivascular mononuclear infiltrates in alveolated lung parenchyma and blood vessels are cuffed by lymphocytes forming a ring of two or three cells in thickness within the perivascular adventitia	Low-grade small airway inflammation without epithelial damage	2
	2	Frequent perivascular mononuclear infiltrates are seen surrounding venules and arterioles and are readily recognizable at low magnification	High-grade small airway inflammation, with individual cell apoptosis, to ulcers to total denudation of epithelium	4

	Score			Total score
	3	Easily recognizable cuffing of venules and arterioles by dense perivascular mononuclear cell infiltrates, associated with endothelialitis		3
	4	Diffuse perivascular, interstitial and air-space infiltrates of mononuclear cells with prominent alveolar pneumocyte damage and endothelialitis		4
Heart [6]	Score	Cardiomyocyte damage		Total score
	0	Normal cardiomyocyte profile		0
	1	Mononuclear cell infiltrates with or without myocyte damage		1
	2	Diffuse mononuclear cell infiltrates forming space-occupying lesion		2
	3	Disruption of normal architecture with polymorphous infiltrates, edema, hemorrhage and vasculitis		3
Liver [7]	Score	Periportal area and centrilobular damage		Total score
	0	Normal, without significant abnormality		0
	1	Mild damage, less than 50% of the portal tracts are involved by inflammation accompanied by bile duct damage and/or endotheliitis		1
	2	Moderate damage, more than 50% of the portal tracts are involved by inflammation accompanied by bile duct damage and/or endotheliitis		2
	3	Severe, centrilobular necrosis and/or significant piecemeal necrosis		3
Kidney [8]	Score	Interstitial inflammatory cell infiltration	Tubulitis and vasculitis	Total score
	0	No inflammatory cell infiltration	No evidence of tubulitis or endothelitis	0
	1	Mild, variable amounts (but often >25%) of the parenchyma contain interstitial infiltrates of small and large (activated) lymphocytes, monocytes, and plasma cells	Tubulitis without evidence of endothelitis	2
	2	Severe, large amounts of the parenchyma contain interstitial infiltrates	Endothelitis of small or, more often, large arteries with or without the tubulitis	4
Brain [9, 10]	Score	Vessels	Brain parenchyma	Total score
	0	Normal	Normal	0
	1	Vasculitis with lymphocytic infiltrations in subendothelium and blood vessel wall	Mild brain edema	2
	2	Vasculitis with lymphocytic infiltrations in perivascular areas	Brain edema and hematoma	4
	3	Affected vessels had hyaline changes and fibrosis, and partial lumen occlusions with organized thrombotic material	Parenchymal ischemia and sporadic focal demyelination and microglia reaction.	6
	4	Aneurysm formation	Parenchymal hemorrhage and mild atrophy	8

References

1.   Ciofu O, Petersen TD, Jensen P, Hoiby N. Avidity of anti-P aeruginosa antibodies during chronic infection in patients with cystic fibrosis. Thorax 1999; 54:141-4.

2.   Saalman R, Dahlgren UI, Fallstrom SP, Hanson LA, Ahlstedt S, Wold AE. Avidity progression of dietary antibodies in healthy and coeliac children. Clinical and Experimental Immunology 2003; 134:328-34.

3.   Ito R, Shin-Ya M, Kishida T, Urano A, Takada R, Sakagami J, et al. Interferon-gamma is causatively involved in experimental inflammatory bowel disease in mice. Clinical and Experimental Immunology 2006; 146:330-8.

4.   McDonald GB SG. The human gastrointestinal tract after allogeneic marrow transplantation. New York: Masson, 1984.

5.   Horn TD, Rest EB, Mirenski Y, Corio RL, Zahurak ML, Vogelsang GB. The significance of oral mucosal and salivary gland pathology after allogeneic bone marrow transplantation. Archives of dermatology 1995; 131:964-5.

6.   Stewart S, Fishbein MC, Snell GI, Berry GJ, Boehler A, Burke MM, et al. Revision of the 1996 working formulation for the standardization of nomenclature in the diagnosis of lung rejection. The Journal of heart and lung transplantation : the official publication of the International Society for Heart Transplantation 2007; 26:1229-42.

7.   Shulman HM, Kleiner D, Lee SJ, Morton T, Pavletic SZ, Farmer E, et al. Histopathologic diagnosis of chronic graft-versus-host disease: National Institutes of Health Consensus Development Project on Criteria for Clinical Trials in Chronic Graft-versus-Host Disease: II. Pathology Working Group Report. Biol Blood Marrow Transplant 2006; 12:31-47.

8.   Solez K, Benediktsson H, Cavallo T, Croker B, Demetris AJ, Drachenberg C, et

al. Report of the Third Banff Conference on Allograft Pathology (July 20-24, 1995) on

classification and lesion scoring in renal allograft pathology. Transplant Proc 1996;

28:441-4.

9.   Campbell JN, Morris PP. Cerebral vasculitis in graft-versus-host disease: a case

report. AJNR American journal of neuroradiology 2005; 26:654-6.

10.   Padovan CS, Bise K, Hahn J, Sostak P, Holler E, Kolb HJ, et al. Angiitis of the

central nervous system after allogeneic bone marrow transplantation? Stroke; a journal

of cerebral circulation 1999; 30:1651-6.

NA = Donor samples were not employed in T cell assays. Rather, this paper explored CAR engineered mouse T cells. Therefore, several sections do not apply. Relevant sections have been completed.

Required	If Available	Optional	
Module 1 - Sample			
Module 1A - Donor			
Required	*If Available*	*Optional*	
☐NA			Essential donor info
Module 1B - Source			
☒			Source of cell material
☒			Collection methodology
	☐		Anti-coagulant, if available
	☐		Transportation/storage conditions for unprocessed samples, if available
☒			Cell processing methodology
	☐		Median time and ranges from sample collection until end of cell processing, if available
	☐		Cut-offs, if used
Module 1C - Cryopreservation and Storage			
☒			Fresh or cryopreserved
			If cryopreserved
☐NA			Devices used
☐NA			Freezing process
☐NA			Medium used for freezing
	☐		Median time and temperature for each transportation and storage step, if available
	☐		Cut-offs, if used
Module 1D - Cell Counting			
☐NA			Median cell yield and viability (when available)
	☐		Before freezing
	☐		After thawing
	☐		After overnight resting
	☐		Cut-offs, if used
☒			Cell counting methodology
		☐	*Additional assessments*

Module 2 - Assay			
Module 2A - Medium/Serum			
Required	*If Available*	*Optional*	
X			Medium/(serum) details
X			Pre-testing info
Module 2B - Assay			
	☐		Treatment procedures of cells prior to assay, if applicable
X			Sufficient assay details
Module 2C - Controls			
X			Internal assay controls
	☐		Acceptance criteria, if available
	☐		External reference samples, if used
	☐		Assay acceptance criteria, if available

Module 3 - Data Acquisition			
Module 3A - Equipment and Software			
Required	*If Available*	*Optional*	
X			Equipment and software version
	☐		Basic equipment settings, if available
Module 3B - Acquisition Strategy and Gating			
X			Detailed gating strategy or strategy for establishing spot detection parameters
X			Representative data set
	X		Mean,median, ranges of event counts for relevant populations, if available
		☐	*Unusual strategies explained*
		☐	*Review of raw data*

Module 4 - Results			
Module 4A - Raw Data			
Required	*If Available*	*Optional*	
	☐		Background and Ag-specific reactivity levels, if available
	☐		Cut-off specifications and # of tests out-of-specification, if available
☒			Accessibility of raw data addressed?
Module 4B - Response Determination			
☐NA			Definition of positive reactivity (above background) including tests applied
	☐		Parameters, software and version used for response determination, if applicable
☐NA			Response definition predefined or post-hoc?
	☐		Definition of response induced by treatment, if applicable
	☐		Any data excluded and why, if applicable?
		☐	*Why test was used*

Module 5			
Module 5A - General Lab Operation			
Required	*If Available*	*Optional*	
☒			Guidance of lab operations
	☐		Laboratory accreditations and certifications, if available
		☐	*Details on audits*
Module 5B - Standardization			
☒			Status of protocols
Module 5C - Qualification/Validation			
☒			Status of assays
		☐	*Specific performance criteria*